ISSN 2580-0817

Simulation-based Methodology to Investigate the Impact of Material Type and Compressive Speed Variation on Effective Strain Rate and Springback

Radhi Nurvian Amrullah*, Syamsul Hadi, Muhammad Akhlis Rizza

Department of Mechanical Engineering, Malang State Polytechnic,
Jl. Soekarno Hatta No. 9, Malang, 65141, Indonesia
**Corresponding author: radhinurvian.rn@gmail.com*

Article history:
Received: 10 July 2024 / Received in revised form: 5 August 2024 / Accepted: 25 August 2024
Available online 1 September 2024

ABSTRACT

To obtain the desired results in the manufacturing process, especially the bending process, the occurrence of springback must be reduced. The effective strain rate must be increased to predict the increase in material. This study uses a simulation method to determine the influence of material type and compressive speed variation on spring back and effective strain rate. This study uses 3 kinds of materials: JIS SPHD, JIS A1100 BE, and JIS SN400A, and speed variations, namely: 90 mm/s, 105 mm/s, and 120 mm/s. This study shows that JIS SN400A material has the smallest springback value compared to JIS A1100 BE and JIS SPHD materials because the nitrogen content in JIS SN400A makes it more plastic. At a compressive speed of 105 mm/s, springbacks tend to decrease in JIS SN400A, JIS SPHD, and JIS A1100 BE materials caused by residual stress. The average effective strain in JIS SN400A material increases in line with the increase in compressive speed, because JIS SN400A material has the highest melting temperature compared to JIS SPHD and JIS A1100 BE materials to reduce the risk of residual stress, the nitrogen content in JIS SN400A material also plays a role in increasing the effective strain value.

Keywords: *Effective strain rate, material, simulation, springback.*

I. Introduction

In the manufacturing process, especially in the bending process, to get the results that suit the needs is a hope for engineers. In the bending process itself, we recognize the existence of springback. Springback is a common phenomenon in sheet metal formation where elastic recovery causes deviations from the intended geometry after load release. This affects the precision and quality of the product, posing challenges in the manufacturing process [1].

In addition, to predict the properties of the material is also important, some possible ways to do it are to know the effective strain rate on the material. The effective strain rate significantly affects the behavior of maintaining material in various materials. In AlN ceramics, the higher scratch speed leads to a finer penetration depth and fewer cracks, encouraging the occurrence of plasticity [2]. For plates, strain rate sensitivity and strain hardening affect the saturation impulse, with displacement inversely proportional to the stiffening factor [3]. In Fe-30Mn-8Al-1.0C austenitic steels, an increase in the strain rate from 10^{-4} to 10^{-1} s^{-1} increases the yield strength, with the optimal strength-ductility combination achieved at 10^{-3} s^{-1} due to the twin-induced microband and plasticity [4]. For A356-T7 cast aluminum alloy, the higher strain rate (10% s^{-1} vs 1% s^{-1}) results in increased

DOI: 10.17977/um016v8i22024p229

isotropic hardening and softening rates, and more failure cycles. Strain rate also had a significant effect on the development of average stress at room temperature. These findings highlight the importance of considering the effects of strain rate in material design and processing [5].

The parameters that are suspected to influence the occurrence of springback and effective strain rate are the type of material to be used and the compression speed. To validate this, simulation methods can be used. Simulation methods are increasingly used in materials testing because of their ability to produce results comparable to physical experiments. Studies have shown that computer simulations of tensile tests on polymer composites can achieve results within 7% of the actual test [6]. Similarly, finite element modeling on shot peening can produce residual stresses equivalent to experimental processes [7]. The digital image correlation method (DICM) has been successfully applied to similar material simulation experiments for rock-like materials, providing a full-field deformation and strain analysis that is perfectly matched to physical tests [8]. In estimating the fatigue life of the cardan shaft components, numerical simulations combining the material-specific stress life curve and surface roughness factors have shown good agreement with the results of physical testing. These studies highlight the effectiveness of simulation methods in materials testing, offering a cost-effective and time-efficient alternative to traditional experimental approaches [9-11].

Car bodies are generally made of steel and aluminum with a manufacturing process in the form of bending, therefore the author took the initiative to conduct research effect of material type and pressing speed on springback using a simulation method on the bending process.

II. Material and Methods

This study uses a simulation method with several parameters, as shown in Table 1.

Table 1. Parameter of simulation

Parameter	Value
Specimen size	2 x 19 x 200 mm
Material of punch	S45C
Material of dies	S45C
Punch angle	90˚
Dies angle	90˚
Radius punch	0.5 mm
Radius dies	1 mm
Temperature punch	20˚
Temperature dies	20˚
Material temperature	20˚
Material Type	JIS SPHD, JIS A1100 BE, JIS SN400A
Press speed	90 mm/s, 105 mm/s, 120 mm/s

This study uses a constant compressive speed variation using hydraulic presses, namely 90 mm/s, 105 mm/s, and 120 mm/s, and uses 3 different types of materials, namely JIS

SPHD, JIS A1100 BE, and JIS SN400A, the following is the material chemical composition used as shown in Table 2.

Table 2. Chemical composition of materials

Element	Chemical Composition (%)		
	JIS SPHD	JIS A1100 BE	JIS SN400A
Al	-	99	-
C	0.19	-	0.15
Fe	98.34	0.5	98.293
Mn	0.3	0.05	1.1
P	0.02	-	0.02
S	0.02	-	0.027
Si	0.2	0.45	-
Cr	0.2	-	-
Cu	0.1	0.2	0.4
N	-	-	0.01
Zn	-	0.1	-

This research process begins by determining the case in the metal forming process, then determining the parameters related to the process, then carrying out the design and simulation process using computer-aided design (CAD) software namely Simufact version 15 in 2018, then the process of taking and analyzing data using Microsoft excel software and finally concluding from the analysis results. This study uses three components, namely punch, sample, and dies, whose size designs are depicted in Figure 1.

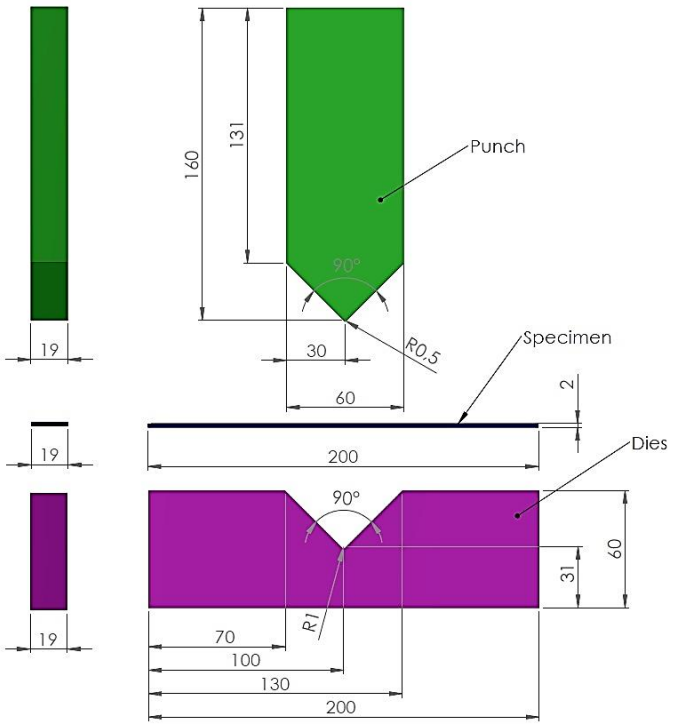

Fig 1. Punch, specimen, and dies sizes

The mechanical properties of the materials used in the simulation software are already available for the materials used in this study, as shown in Table 3.

Table 3. Mechanical properties of the material in a CAD software database

	Mechanical properties of material			
	JIS SPHD	JIS A1100 BE	JIS SN400A	S45C
Tensile strength (MPa)	608	89.6	400	686
Yield strength (MPa)	438	34.4	235	490

For this study, the mesh used using the automatic method of the software was 0.679628 mm in size, as shown in Figure 2.

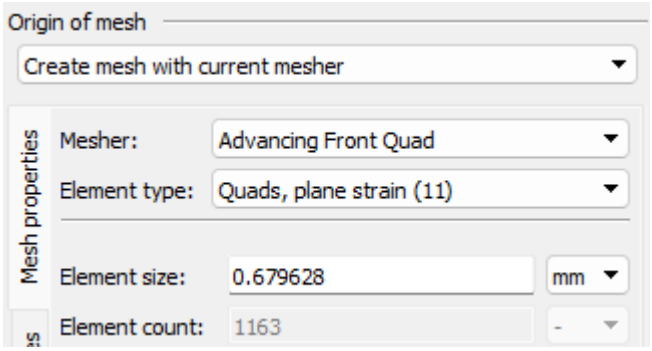

Fig 2. Mesh size

The following simulation modeling is shown in Figure 3.

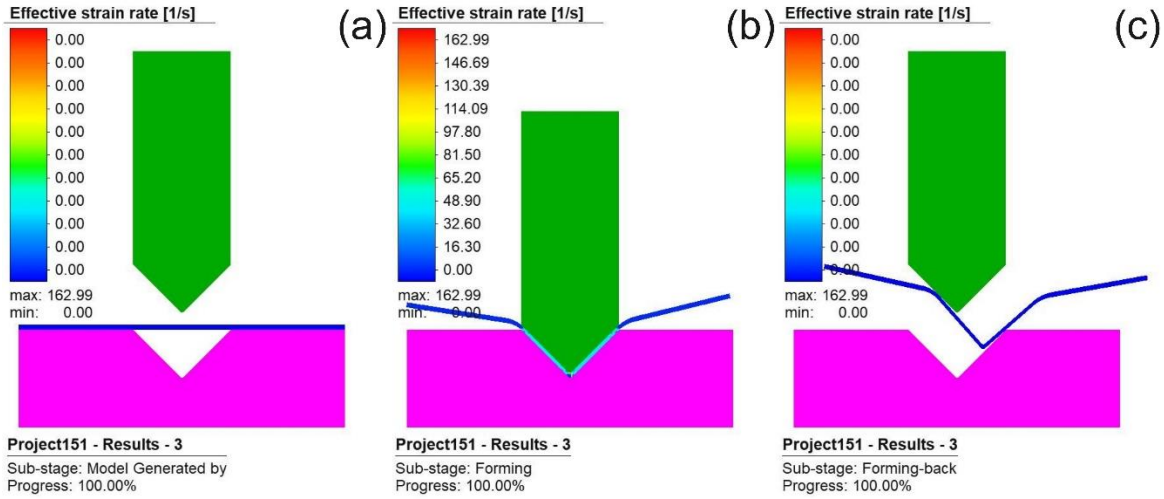

Fig. 3. Simulation modeling steps : (a) The punch is moved towards the specimen, (b) The punch presses the specimen, and (c) The punch returns to its original position.

In the simulation process, several parameters such as effective strain rate are generally available in CAD software, but for springback, there is still no springback, so to find out the springback, image analysis software is used. The hydraulic punch is moved downward at a constant speed to start the simulation process (a), next, the punch presses the specimen to form an angle based on the dies' shape; from this simulation step, the effective strain rate

parameter data is obtained (b), finally, the punch returns to its original position after pressing the specimen, causing springback in the specimen (c), as depicted in Figure 3. The process of determining the springback begins by inputting the simulation image and then inputting it into the software, then the springback data is taken 3 repetitions and taken on average from the springback. Then the result is reduced by the size of the die angle, in this study, the size of the die angle is 90˚ so that the springback size is obtained. Figure 4 shows the springback data collection was carried out in 3 iterations because the images produced were not of good quality, so it is hoped that the data collection of 3 iterations can validate the results that are closest to the actual situation. The steps are to add a line to the bottom of the specimen as an auxiliary line (a), this line does not have a standard length because it only functions as an auxiliary line, then make an angle from any point along the auxiliary line so that the angle size of the specimen is obtained (b). The software does not currently have a facility to calculate the duration of the simulation, so the approximate 4-minute simulation time was determined by hand calculations.

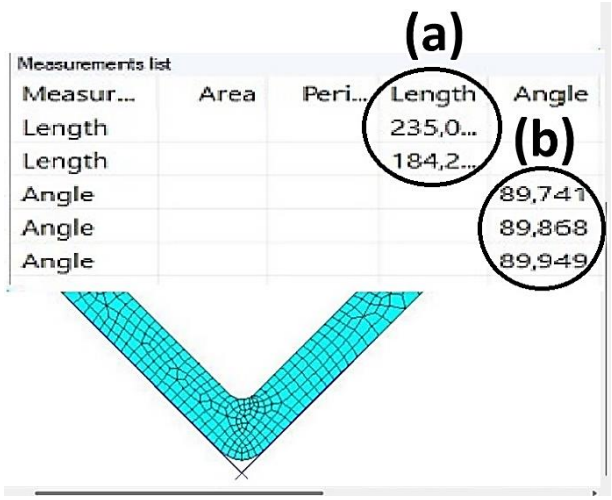

Fig. 4. Springback information recovery process : (a) The auxiliary line added to the bottom of the specimen, and (b) The resulting bending angle formed from the auxiliary line.

III. Results and Discussions

The simulation process is carried out 9 times based on the parameters determined in Table 1 and the simulation results are shown in Table 4. Based on Table 4, it can be seen that the highest springback value of 0.265° occurs in JIS SN400A material with a compressive speed of 90 mm/s, and the lowest of -0.015° occurs in JIS SPHD material with a compressive speed of 90 mm/s. This shows that the most effective parameter in reducing the occurrence of springback is JIS SN400A material and the compressive speed is 105 mm/s because it has the smallest springback value. Whereas a negative spring back value indicates that the specimen cannot return to its original form (the angle curve result is equal to or smaller than the angle size of dies) and that the specimen is more plastic than those with a positive springback value. A positive springback value indicates that the specimen has a spring back to the re-form (angle curvature greater than the angle size of the dies).

Table 4. Result of springback simulation

Material	Press speed (mm/s)	Angle (˚)			Mean	Springback (˚)			Mean
		I	II	III		I	II	III	
JIS SPHD	90	89.955	89.931	90.068	89.984	-0.045	-0.069	0.068	-0.015
	105	89.888	89.885	89.671	89.814	-0.112	-0.115	-0.329	-0.185
	120	89.741	89.868	89.949	89.852	-0.259	-0.132	-0.051	-0.147
JIS A1100 BE	90	90.14	89.988	89.922	90.016	0.14	-0.012	-0.078	0.016
	105	89.92	90.253	89.866	90.013	-0.08	0.253	-0.134	0.013
	120	90.056	90.204	90.210	90.156	0.056	0.204	0.21	0.156
JIS SN400A	90	90.194	90.282	90.320	90.265	0.194	0.282	0.32	0.265
	105	89.481	89.585	89.707	89.591	-0.519	-0.415	-0.293	-0.409
	120	90.051	90.201	90	90.084	0.051	0.201	0	0.084

Based on Figure 5, the dominant decrease in springback value occurs at a compressive speed of 105 mm/s, this is due to the occurrence of residual stress due to an increase in temperature at a compressive speed of 105 mm/s (generally the compressive speed on the test machine is 0.08 mm/s) to affect the resulting product [12-15]. JIS A1100 BE material has the highest average springback value, while JIS SN400A material has the lowest average springback value, this is because aluminum has better elastic properties than steel and the nitrogen content in JIS SN400A material causes its mechanical properties to be more plastic as shown in Table 2 [16-23]. As Table 5 shows, the traction strength of the AISI 304 L steel increases with the level of nitrogen.

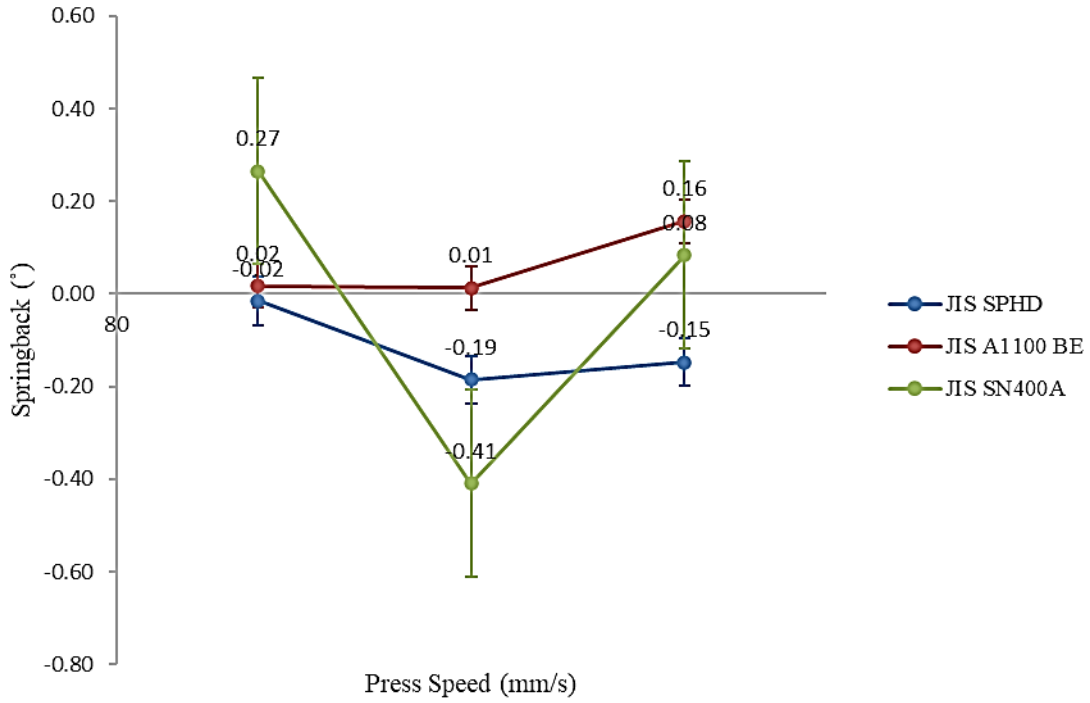

Fig. 5. Graph of springback simulation results

Table 5. Chemical composition and tensile strength of AISI 304L [18]

Grade	Chemical composition, wt.%						Tensile strength (MPa) after heat treatment	
							Quenching,30 min water	
	C	Si	Mn	Cr	Ni	N	1050˚C	1100˚C
03Cr18Ni11 (AISI 304L) Prototype	0.02	0.65	0.95	18.34	11.07	0.05	560	545
04Cr18Ni11 Mn1N0.16	0.04	0.56	1.35	18.3	11.11	0.16	674	635
03Cr18Ni11 Mn1N0.16	0.03						651	639
05Cr19Ni9 Mn3N0.21	0.05	0.47	2.95	19.62	9.65	0.21	726	725
03Cr20Ni9 Mn3N0.27	0.03			20.3		0.27	756	753
06Cr19Ni9 Mn3N0.23	0.06	0.41	3.02	19.63	9.6	0.23	746	721
03Cr20Ni9 Mn3N0.30	0.03	0.3		20.26		0.3	777	744

Table 6 shows that JIS SN400A material has the highest effective strain rate value of 1801.22 1/s with a compressive velocity of 120 mm/s, and JIS SPHD material has the lowest effective strain rate value of 238.33 1/s with a compressive speed of 105 mm/s. This shows that, because it has the highest effective strain rate value, the JIS SN400A material is the most effective for producing more strength [24-26].

Table 6. Result of effective strain rate simulation

Material	Press speed (mm/s)	Effective strain rate (1/s)
JIS SPHD	90	681.01
	105	797.77
	120	719.67
JIS A1100 BE	90	1109.75
	105	238.33
	120	339.32
JIS SN400A	90	1350.92
	105	1576.07
	120	1801.22

Based on Figure 6, the effective strain rate value increases in line with the increase in the compressive speed of JIS SN400A material, this material has the highest effective strain rate value compared to JIS SPHD and JIS A1100 BE materials, this is because JIS SN400A material has the highest melting point (1520° C) compared to JIS SPHD (1480° C) and JIS A1100 BE (657° C) materials, As the table 7 shows, the higher the material temperature, the more the effective strain rate value increases [27-30]. The nitrogen content in JIS SN400A

material as shown in Table 2, also plays a role in increasing the effective strain rate value [31-34].

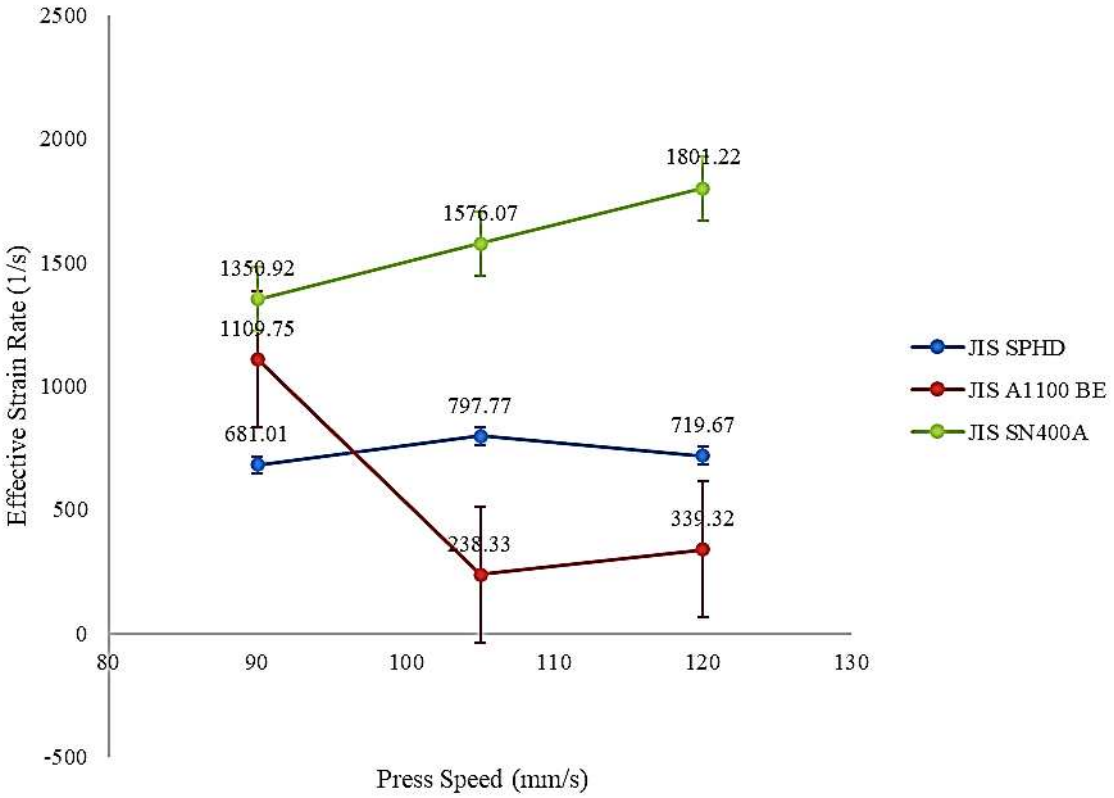

Fig. 6. Graph of effective strain rate simulation results

Table 7. Effective Strain Rate at different temperatures [27]

Material		Molybdenum-L
Test	Temperature	Effective Strain Rate (1/s)
Test 1	273	1151
Test 2	473	3700
Test 3	673	8500
Test 4	873	3000
Test 5	1073	7499
Test 6	1273	3500

IV. Conclusions

This study aims to determine the effect of material type and compression speed on springback and effective strain value. This study shows that JIS SN400A material has the smallest springback value compared to JIS A1100 BE and JIS SPHD materials, because the nitrogen content in JIS SN400A makes it more plastic, and at a compression speed of 105 mm/s, springback tends to decrease in JIS SN400A, JIS SPHD, and JIS A1100 BE materials caused by residual stress. The average effective strain in JIS SN400A material increases with increasing compression speed because JIS SN400A material has the highest melting

temperature compared to JIS SPHD and JIS A1100 BE materials, the nitrogen content in JIS SN400A material also plays a role in increasing the effective strain value. In future prospects, the results of this study can be used to reduce the occurrence of springback in the bending process, with the bending speed specification must be constant and determined during the manufacturing process.

Acknowledgment

The author is grateful for the assistance in financing DIPA funds by the Malang State Polytechnic.

References

[1] P. Mulidrán, E. Spišák, M. Tomáš, J. Slota, and J. Majerníková, 'Numerical prediction and reduction of hat-shaped part springback made of dual-phase AHSS steel', *Metals (Basel)*, vol. 10, no. 9, p. 1119, Aug. 2020, doi: 10.3390/met10091119.

[2] S. Gao, H. Li, R. Kang, Y. Zhang, and Z. Dong, 'Effect of strain rate on the deformation characteristic of AlN ceramics under scratching', *Micromachines (Basel)*, vol. 12, no. 1, p. 77, Jan. 2021, doi: 10.3390/mi12010077.

[3] L. Zhu, X. He, F. L. Chen, and X. Bai, 'Effects of the strain rate sensitivity and strain hardening on the saturated impulse of plates', *Latin American Journal of Solids and Structures*, vol. 14, no. 7, pp. 1273–1292, Aug. 2017, doi: 10.1590/1679-78253664.

[4] J. Du, P. Chen, X. Guan, J. Cai, Q. Peng, C. Lin et al., 'The effect of strain rate on the deformation behavior of Fe-30Mn-8Al-1.0C austenitic low-density steel', *Metals (Basel)*, vol. 12, no. 8, p. 1374, Aug. 2022, doi: 10.3390/met12081374.

[5] E. Natesan, J. Ahlström, S. K. Manchili, S. Eriksson, and C. Persson, 'Effect of strain rate on the deformation behaviour of A356-T7 cast aluminium alloys at elevated temperatures', *Metals (Basel)*, vol. 10, no. 9, p. 1239, Sep. 2020, doi: 10.3390/met10091239.

[6] A. Śliwa, W. Kwaśny, M. Nabia, and R. Dziwis, 'Numerical analysis of static tensile test of the sample made of polyethylene reinforced by halloysite nanoparticles', *Acta Phys Pol A*, vol. 136, no. 6, pp. 996–1000, Dec. 2019, doi: 10.12693/APhysPolA.136.996.

[7] M.R. Isa, S.N. Sulaiman, and O.S. Zaroog, 'Experimental and simulation method of introducing compressive residual stress in ASTM A516 grade 70 steel', *Key Eng Mater*, vol. 803, pp. 27–31, May 2019, doi: 10.4028/www.scientific.net/KEM.803.27.

[8] H. Kong, L. Wang, G. Gu, and B. Xu, 'Application of DICM on similar material simulation experiment for rock-like materials', *Advances in Civil Engineering*, vol. 2018, pp. 1–15, Apr. 2018, doi: 10.1155/2018/5634109.

[9] M. Ozbakiş, E. C. Yeni, and M. C. Kahyalar, 'Investigation of the similarity between physical tests and fatigue simulation of flange yoke made of C45 E material used in cardan shafts', *Materwiss Werksttech*, vol. 53, no. 7, pp. 798–807, Jul. 2022, doi: 10.1002/mawe.202000257.

[10] R. Prasetya, A. Andoko, S. Suprayitno, R. Wulandari, P. Trihutomo, K. Mishima et al., 'Simulation of the performance of kevlar impregnated shear thickening fluid ballistic test results (STF) ballistic test results', *Journal of Mechanical Engineering Science and Technology*, vol. 8, no. 1, p. 54, May 2024, doi: 10.17977/um016v8i12024p054.

[11] D. Z. Lubis and A. Andoko, 'Elastic linear analysis of connecting rods for single cylinder four stroke petrol engines using finite element method', *Journal of*

Mechanical Engineering Science and Technology, vol. 3, no. 1, pp. 42–50, Aug. 2019, doi: 10.17977/um016v3i12019p042.

[12] V. Taşdemir, 'Finite element analysis of the springback behavior after V bending process of sheet materials obtained by Differential Speed Rolling (DSR) method', *Revista de Metalurgia*, vol. 58, no. 1, p. e219, Jul. 2022, doi: 10.3989/revmetalm.219.

[13] H.A.J. Hiseeb and A.A. Khleif, 'Experimental investigations of a springback in hydromechanical deep drawing of low carbon steel 1008 AISI', *Tikrit Journal of Engineering Sciences*, vol. 31, no. 2, pp. 20–27, Apr. 2024, doi: 10.25130/tjes.31.2.3.

[14] J. Styks, A. Knapczyk, and B. Łapczyńska-Kordon, 'Effect of compaction pressure and moisture content on post-agglomeration elastic springback of pellets', *Materials*, vol. 14, no. 4, p. 879, Feb. 2021, doi: 10.3390/ma14040879.

[15] T.-C. Chen, S.-X. Chen, C.-C. Wang, and T.-E. Lee, 'Analysis of the punch motion curve for the springback of U-shaped sheet metal', *Advances in Mechanical Engineering*, vol. 15, no. 3, p. 168781322311611, Mar. 2023, doi: 10.1177/16878132231161151.

[16] Y. Fan, J. Zhou, J. Gu, H. Chi, D. Ma, and G. Xie, 'Effect of N on the microstructure and wear resistance of 4Cr13 corrosion-resistant plastic mold steel', *Materials*, vol. 17, no. 2, p. 308, Jan. 2024, doi: 10.3390/ma17020308.

[17] G. Chai, R. Siriki, J. Nordström, Z. Dong, and L. Vitos, 'Roles of nitrogen on TWIP in advanced austenitic stainless steels', *Steel Res Int*, vol. 94, no. 10, Oct. 2023, doi: 10.1002/srin.202200359.

[18] F. Shi, X. Zhang, T. Li, X. Guan, X. Li, and C. Liu, 'Effects of Nitrogen content and strain rate on the tensile behavior of high-nitrogen and nickel-free austenitic stainless steel', *Crystals (Basel)*, vol. 13, no. 1, p. 129, Jan. 2023, doi: 10.3390/cryst13010129.

[19] V. Shabashov, K. Lyaskov, K. Kozlov, V. Zavalishin, A. Zamatovskii, V. Sagaradze *et al.*, 'Critical redistribution of nitrogen in the austenitic Cr-Mn steel under severe plastic deformation', *Materials*, vol. 14, no. 23, p. 7116, Nov. 2021, doi: 10.3390/ma14237116.

[20] A.N. Maznichevsky, R.V. Sprikut, and Y.N. Goikhenberg, 'Investigation of nitrogen containing austenitic stainless steel', *Materials Science Forum*, vol. 989, pp. 152–159, May 2020, doi: 10.4028/www.scientific.net/MSF.989.152.

[21] A. Sharma, S. K. Yadav, A. Yadav, V. Kumar, and A. Kumar, 'Comparison of static and harmonic response of structural steel and aluminium alloy automotive shock absorbers', 2021, pp. 241–249. doi: 10.1007/978-981-16-0909-1_24.

[22] S. Sudirman, V. Vegisari, H. Kuswanto, and E. Rudiansyah, 'Spreadsheet to analyze the comparative of elasticities properties of aluminum alloy materials', *Jurnal Riset dan Kajian Pendidikan Fisika*, vol. 10, no. 1, pp. 16–21, Apr. 2023, doi: 10.12928/jrkpf.v10i1.224.

[23] A. Kumar, R. Maithani, A. Kumar, D. Kumar, and S. Sharma, 'An all-aluminium vehicle's design and feasibility analysis', *Mater Today Proc*, vol. 64, pp. 1244–1249, 2022, doi: 10.1016/j.matpr.2022.03.714.

[24] T. Taylor, S. Danks, and G. Fourlaris, 'Dynamic tensile testing of ultrahigh strength hot stamped martensitic steels', *Steel Res Int*, vol. 88, no. 3, p. 1600144, Mar. 2017, doi: 10.1002/srin.201600144.

[25] J. Du, P. Chen, X. Guan, J. Cai, Q. Peng, C. Lin et al., 'The effect of strain rate on the deformation behavior of Fe-30Mn-8Al-1.0C austenitic low-density steel', *Metals (Basel)*, vol. 12, no. 8, p. 1374, Aug. 2022, doi: 10.3390/met12081374.

[26] M. Pitoňák, J. Ondruš, K. Zgútová, M. Neslušan, and J. Moravec, 'Influence of strain rate on plastic deformation of the flange in steel road barrier', *Materials*, vol. 16, no. 4, p. 1396, Feb. 2023, doi: 10.3390/ma16041396.
[27] L. Kyzioł, 'Dynamic properties of 40HM steels at high strain rates', *Transactions of FAMENA*, vol. 43, no. 4, pp. 55–68, Feb. 2020, doi: 10.21278/TOF.43405.
[28] P. Song, W.-B. Li, Y. Zheng, J.-P. Song, X.-C. Jiang, and B.-Y. Yan, 'Study on plastic deformation behavior of Mo-10Ta under ultra-high strain rate', *Metals (Basel)*, vol. 10, no. 9, p. 1153, Aug. 2020, doi: 10.3390/met10091153.
[29] S. Chen, W. Li, X. Wang, W. Yao, J. Song, X. Jiang et al., 'Comparative study of the dynamic deformation of pure molybdenum at high strain rates and high temperatures', *Materials*, vol. 14, no. 17, p. 4847, Aug. 2021, doi: 10.3390/ma14174847.
[30] N.V. Melekhin, 'A model of microstructure evolution under high-strain rate deformation of copper', *Problems of Strength and Plasticity*, vol. 85, no. 2, pp. 178–188, 2023, doi: 10.32326/1814-9146-2023-85-2-178-188.
[31] F. Shi, X. Zhang, T. Li, X. Guan, X. Li, and C. Liu, 'Effects of Nitrogen Content and Strain Rate on the Tensile Behavior of High-Nitrogen and Nickel-Free Austenitic Stainless Steel', *Crystals (Basel)*, vol. 13, no. 1, p. 129, Jan. 2023, doi: 10.3390/cryst13010129.
[32] Z. Baochun, Z. Tan, L. Guiyan, and L. Qiang, 'Effect of nitrogen on the dynamic recrystallization behaviors of vanadium and titanium microalloyed steels', *Archives of Metallurgy and Materials*, Feb. 2018, doi: 10.24425/118951.
[33] G. Chai, R. Siriki, J. Nordström, Z. Dong, and L. Vitos, 'Roles of nitrogen on TWIP in advanced austenitic stainless steels', *Steel Res Int*, vol. 94, no. 10, Oct. 2023, doi: 10.1002/srin.202200359.
[34] F. Stern, L. Becker, C. Cui, J. Tenkamp, V. Uhlenwinkel, M. Steinbacher et al., 'Improving the defect tolerance of PBF-LB/M processed 316L steel by increasing the nitrogen content', *Adv Eng Mater*, vol. 25, no. 1, Jan. 2023, doi: 10.1002/adem.202200751.